Published in final edited form as:
*Neuroimage*. 2012 November 15; 63(3): 1060–1069. doi:10.1016/j.neuroimage.2012.08.025.

# Finding Thalamic BOLD Correlates to Posterior Alpha EEG

**Zhongming Liu**[*], **Jacco A. de Zwart**, **Bing Yao**, **Peter van Gelderen**, **Li-Wei Kuo**, and **Jeff H. Duyn**
Advanced Magnetic Resonance Imaging Section, Laboratory of Functional and Molecular Imaging, National Institute of Neurological Disorders and Stroke, National Institutes of Health, Bethesda, MD, USA

## Abstract

Oscillatory electrical brain activity in the alpha (8–13Hz) band is a prominent feature of human electroencephalography (EEG) during alert wakefulness, and is commonly thought to arise primarily from the occipital and parietal parts of the cortex. While the thalamus is considered to play a supportive role in the generation and modulation of cortical alpha rhythms, its precise function remains controversial and incompletely understood. To address this, we evaluated the correlation between the blood oxygenation level dependent (BOLD) functional magnetic resonance imaging (fMRI) signals in the thalamus and the spontaneous modulation of posterior alpha rhythms based on EEG-fMRI data acquired concurrently during an eyes-closed task-free condition. We observed both negative and positive correlations in the thalamus. The negative correlations were mostly seen within the visual thalamus, with a preference for the pulvinar over lateral geniculate nuclei. The positive correlations were found at the anterior and medial dorsal nuclei. Through functional connectivity analysis of the fMRI data, the pulvinar was found to be functionally associated with the same widespread cortical visual areas where the fMRI signals were negatively correlated with the posterior alpha modulation. In contrast, the dorsal nuclei were part of a distinct functional network that included brain stem, cingulate cortex and cerebellum. These observations are consistent with previous animal electrophysiology studies and the notion that the visual thalamus, and the pulvinar in particular, is intimately involved in the generation and spontaneous modulation of posterior alpha rhythms, facilitated by its reciprocal and widespread interaction with the cortical visual areas. We further postulate that the anterior and medial dorsal nuclei, being part of the ascending neuromodulatory system, may indirectly modulate cortical alpha rhythms by affecting vigilance and arousal level.

### Keywords

EEG-fMRI; Alpha; Thalamus; Pulvinar; Lateral Geniculate Nucleus

## INTRODUCTION

In human EEG, alpha activity (i.e. electrical activity in the 8–13Hz frequency range) is most prominent in occipital and parietal regions when the subject is resting wakefully with eyes closed, and is suppressed with opening of the eyes (Berger, 1929) or falling into sleep



[*]Correspondence: Zhongming Liu, PhD, Advanced MRI Section, LFMI, NINDS, NIH, Building 10, Room B1D-723, 9000 Rockville Pike – MSC 1065, Bethesda, Maryland 20982-1065, Phone: +1 301 451 9915, Fax: +1 301 480 1981, liuz5@mail.nih.gov.

(Niedermeyer, 1997). The occipital dominance of alpha-band EEG activity is thought to reflect primarily cortical dendritic activity synchronized across a large part of the visual cortex, which is situated in the occipital lobe. The neural circuitry underlying this synchronization has not been firmly established and likely includes not only cortico-cortical but also thalamo-cortical connections. Specifically, the involvement of the thalamus remains difficult to assess non-invasively with scalp-recorded EEG alone due to its very low sensitivity to signal sources situated deeper in the brain as is the thalamus.

Invasive electrophysiological recordings from animals have shed light on an important role of the visual thalamus in the generation, modulation and synchronization of alpha rhythms observed from the visual cortex (Hughes and Crunelli, 2005). During natural wakefulness, local field potentials (LFP) recorded from the visual cortex of dogs and cats exhibit robust oscillatory activity centered at 10Hz (Chatila et al., 1993; Lopes da Silva et al., 1973; Lorincz et al., 2009). Like the human posterior alpha rhythm, its amplitude was shown to react in a similar fashion to opening and closing the eyes (Chatila et al., 1992). Importantly, alpha oscillations were also observed specifically within the visual thalamus, including both the lateral geniculate nucleus (LGN) and pulvinar (Pul). Comparison between the alpha rhythms recorded from the thalamic and cortical parts of the animal visual system showed a strong degree of phase-locking and covarying amplitudes (Chatila et al., 1993; Lopes da Silva et al., 1973; Lopes da Silva et al., 1980; Lorincz et al., 2009). In addition, coherence analysis after simulated removal of the visual thalamus by parceling out its contributions to thalamo-cortical synchrony showed a significant decrease of intra-cortical alpha coherence (Lopes da Silva et al., 1980).

Extrapolating these findings from animals to humans, one may hypothesize that the reciprocal (i.e. feedforward and feedback) interactions between the visual thalamus and the visual cortex give rise to the human posterior alpha rhythm. A unique and non-invasive approach to test this hypothesis is to use concurrently recorded fMRI-EEG to search the entire brain for metabolic and/or hemodynamic correlates of the posterior alpha rhythm. This approach benefits from the whole brain coverage and relatively high spatial resolution provided by fMRI. Utilizing this approach, several groups have assessed the correlation between simultaneously acquired BOLD fMRI and alpha EEG primarily in the absence of overt subject activity (de Munck et al., 2007; Feige et al., 2005; Goldman et al., 2002; Laufs et al., 2003; Moosmann et al., 2003; Sadaghiani et al., 2010). Likewise, other groups combining positron emission tomography (PET) and EEG have also attempted to localize changes in regional cerebral blood flow (CBF) and cerebral glucose metabolic rate (CMRglu) that were correlated with the variation of alpha amplitude or power (Buchsbaum et al., 1984; Danos et al., 2001; Larson et al., 1998; Lindgren et al., 1999; Sadato et al., 1998). The results from these studies were generally consistent in cortical regions but notably variable in the thalamus. The correlation between the posterior alpha modulation and the BOLD, CBF or CMRglu signal in the thalamus has been reported to be positive (Danos et al., 2001; de Munck et al., 2007; Feige et al., 2005; Goldman et al., 2002; Moosmann et al., 2003; Sadaghiani et al., 2010; Sadato et al., 1998), negative (Larson et al., 1998; Lindgren et al., 1999; Moosmann et al., 2003) or near-zero (Laufs et al., 2003), as opposed to more reliably negative correlations in the visual cortex reported in most of these studies, except one (Laufs et al., 2003).

One possible source for the discrepancies among these studies relates to the structural and functional heterogeneity of the thalamus. Based on histology (Morel et al., 1997), the thalamus can be divided in a number sub-regions (often called nuclei), many of which have been shown to serve specific functions (Sherman and Guillery, 2006). Numerous tracing studies in animals (Jones, 2007) have demonstrated uniquely specific connectional patterns of thalamic nuclei with cortical functional areas; in humans, this specificity has been

confirmed with tract-tracing based on diffusion MRI (Behrens et al., 2003; Johansen-Berg et al., 2005), resting-state fMRI (Zhang et al., 2008) as well as by a recent electrophysiological study (Elias et al., 2012). For this reason, it is quite possible that individual thalamic sub-regions may also bear a unique relationship with alpha activity. Unfortunately, none of the previous neuroimaging studies was able to register its EEG-fMRI or EEG-PET correlation results to specific thalamic sub-regions, in part due to an inability to localize them to specific thalamic sub-regions (e.g. LGN and Pul). Therefore, the precise nature of thalamic involvement in cortical alpha signals in humans remains poorly understood.

Toward filling this gap, we revisited the sub-cortical and cortical correlations between BOLD fMRI and alpha EEG using recent technical advances for artifact removal from concurrent fMRI-EEG recordings (Liu et al., 2012), high-field anatomical MRI (Duyn et al., 2007), physiological noise correction (Birn et al., 2008; Chang et al., 2009) and functional to structural image alignment (Saad et al., 2009). We aimed to answer a) whether BOLD signals within the visual thalamus were correlated (either negatively or positively) with the spontaneous modulation of posterior alpha rhythms, b) if so, to which sub-regions of the visual thalamus (LGN or Pul) these correlations localized. To address the latter, the reference locations of LGN and Pul were respectively defined using a functional localizer with visual stimulation and high-resolution anatomical imaging, in addition to the use of a histology-based atlas of the thalamus (Morel, 2007). We also evaluated the intrinsic functional connectivity between the thalamus and the cortex to test whether those alpha-correlated thalamic and cortical regions would constitute a coherent functional network.

## METHODS AND MATERIALS

### Experimental Design

In order to localize the neural circuitry underlying spontaneous modulation of posterior alpha rhythms, we measured simultaneous EEG and fMRI signals from 15 healthy volunteers under various experimental conditions and computed the correlation between the BOLD signal and the occipital EEG power at each volunteer's specific alpha frequency. The validity of this approach is based on the assumption that changes in alpha power have a metabolic correlate that leads to a BOLD effect through neurovascular coupling.

Three separate runs were performed to find the BOLD correlate to EEG alpha power, to measure an individual alpha frequency for each subject, and to functionally localize the LGN. Specifically, each subject was instructed to perform the following three tasks: 1) rest wakefully with eyes closed for 10 minutes, 2) rest while alternatingly keeping eyes closed or open in a self-paced manner (about 30 seconds for each period and four minutes in total), and 3) view checkerboard-patterned stimuli (full-screen, black-and-white, 6Hz reversal frequency) presented with a block design (30 s on and 30 s off repeated for three cycles) combined with a continuous fixation task (pressing a button to report random color changes of a central dot). Some subjects participated in multiple scans of the same protocol on the same or different day. At the end of each 10-min resting session, we explicitly asked the subject for feedback about his/her ability to stay wakeful during the entire scan. The session was excluded from further analysis if the subject reported falling asleep or feeling drowsy or if excessive head motion was observed. In total, this study included 35 scans for eyes-closed rest, 21 scans for the eyes-closed-eyes-open task and 21 scans for the visual stimulation.

Note that the use of visual stimulation was to functionally localize LGN for the comparison with the thalamic regions where the BOLD signals were negative correlated with posterior alpha power. This comparison was free of potential errors or biases in the functional-structural image registration or functional-histological registration.

To co-register functionally defined regions (e.g. alpha-BOLD correlated areas) to specific thalamic nuclei, we also performed high-resolution structural imaging based on GRE phase data and used a histology-based atlas of the thalamus. The former was used to describe the in vivo anatomical contrast and details, while the latter was used to identify the name of the nuclei underlying the thalamic alpha-BOLD correlation.

Environmental light exposure was minimized throughout the experiment. All of the subjects had normal or corrected-to-normal vision and gave informed written consent in accordance with a protocol approved by the Institutional Review Board of the National Institute of Neurological Disorders and Stroke at the National Institutes of Health.

## Data Acquisition

We acquired concurrent EEG (32-channel EEG, international 10–20 montage, two unipolar electrodes for electrocardiogram (ECG) and electrooculography (EOG), 16-bit BrainAmp MR, BrainProducts GmbH, Germany) and BOLD fMRI using a single-shot gradient echo (GRE) echo-planar imaging (EPI) sequence on a 3 T Signa MRI system (General Electric Health Care, Milwaukee, WI, USA) equipped with a 16-channel receive-only coil array (NOVA Medical, Wilmington, MA, USA).

Continuously acquired EEG data were referenced to the FCz channel and sampled at 5 kHz with a resolution of 0.5 μV/bit and an analog bandwidth from 0.1 to 250 Hz. The EEG sampling clock was synchronized with an external reference signal extracted from the 10 MHz master clock of the MRI scanner. The onset time of every EPI slice acquisition was also recorded based on a 5 V TTL signal from the scanner. Cardiac and respiratory signals were recorded using a pulse oximeter on the left index finger and a pneumatic belt around the upper abdomen, respectively.

The GRE-EPI data were acquired with 90° flip angle (FA), 30 ms echo time (TE), 1.5 s repetition time (TR), 30 axial slices with 4 mm thickness and no inter-slice gap, $220\times165 mm^2$ field of view (FOV) for 64×48 matrix and sensitivity encoding (SENSE) parallel imaging with an acceleration factor of two (rate-2) as described earlier (de Zwart et al., 2002). The last imaging volume was acquired with slightly longer TE to measure the spatial variation of the $B_0$ field. $T_1$-weighted anatomical images covering the whole head were acquired with 3-D magnetization prepared rapid gradient echo (3-D MPRAGE) (FA=12°, TE=2.25 ms, TR=5 ms, inversion time = 725 ms, 200 sagittal slices, 1 $mm^3$ isotropic resolution, rate-2 SENSE).

From 10 subjects, $T_2$*-weighted magnitude and phase images were also acquired with 2-D multi-echo GRE (rate-2 SENSE, TE=15.5/30/40.5 ms, TR=2 s, 90 axial slices with $0.31\times0.31$ $mm^2$ in-plane resolution, 0.8 mm slice thickness and 0.2mm gap) using a 7 T Signa MRI system (General Electric Health Care, Milwaukee, WI, USA) with a 32-channel receive coil array (NOVA Medical, Wilmington, MA, USA). We did not select subjects for the 7T MRI. The 7T scans were not specifically for the purpose of this study, but happened to cover 10 subjects included in the subject pool of this study. The uncovered subjects are not available for the 7T scan, as our GE 7T scanner has been removed from the facility.

## Data Preprocessing

EEG artifacts related to MRI gradient switching and cardiac pulsation were removed by using a Matlab-based toolbox as described in (Liu et al., 2012). The EEG signals were then band-pass filtered from 0.5 to 70 Hz and down-sampled to 250 Hz. Independent component analysis (ICA) was further applied to the EEG data in order to remove artifacts related to eye and muscle activities, which were identified through visual inspection of the time course and spatial pattern of individual components.

Geometric distortion in fMRI images was corrected using the $B_0$ field map measured with EPI. Physiological motion effects related to cardiac and respiratory cycles were removed on a slice-by-slice basis by using a retrospective image-based correction method (RETROICOR) as described elsewhere (Glover et al., 2000). The time series of EPI images were corrected for slice timing difference and realigned to the first volume to account for subtle head motion by using FSL (FMRIB, Oxford, UK) (Smith et al., 2004). Linear regression was then performed to remove nuisance variables including a third-order polynomial function modeling the slow signal drift and two additional regressors derived from variations in respiratory volume per time (RVT) and heart rate (HR) using two model-based methods described in (Birn et al., 2008) and (Chang et al., 2009), respectively. Spatial smoothing was then applied by using a 3-D Gaussian kernel with 4 mm isotropic full width at half maximum (FWHM). An improved method for $T_2$*-to-$T_1$ weighted image alignment (Saad et al., 2009), using align_epi_anat.py in AFNI (NIMH, NIH, USA) (Cox, 1996), was used to register the EPI images to the MPRAGE images with a rigid-body transformation. This method was beneficial for the present study, providing an accurate alignment of internal brain structures (e.g. the thalamus) between the functional and structural images for every individual subject. The structural images were further transformed to the standard Montreal Neurological Institute (MNI) stereotactic space using a nonlinear registration tool (FNIRT) in FSL. This nonlinear transformation was saved for the subsequent normalization of functional images or maps from individuals' brain to the MNI space for group analysis (to be explained as below).

### Alpha-BOLD Correlation

For each subject, the individual alpha frequency (IAF) was determined based on the greatest spectral contrast within the alpha band between the eyes-closed and eyes-open periods, using a 0.2-Hz spectral resolution. During the eyes-closed rest, the temporal power fluctuation at IAF was extracted from the spectrogram (i.e. EEG power as a function of time and frequency) computed with a 2 s time window sliding in 1 s steps. The spectrogram was estimated with 0.5 Hz spectral resolution by using a multitaper algorithm implemented in Chronux (Mitra and Bokil, 2008). The posterior alpha modulation was obtained by averaging the alpha power signals extracted from three occipital electrodes (O1, O2 and Oz). An alpha regressor was derived from the convolution of the posterior alpha power with a canonical hemodynamic response function (HRF) in SPM8 (Wellcome Trust Centre for Neuroimaging, University College London, UK). The same nuisance variables (including RVT and HR) excluded from the fMRI signals were also regressed out from the alpha regressor. After that, the alpha regressor was correlated with the BOLD signals throughout the brain. The resulting correlation coefficients were converted to z-values using the Fisher's r-to-z transform. After normalizing the z-map to the MNI space, the alpha-BOLD correlation was first averaged across multiple sessions for the same subject. Then individual subjects' results were averaged and tested for the group-level statistical significance using one-sample t-test (3dttest++ in AFNI). The t-threshold was chosen such that the false discovery rate, denoted as q, was less than 0.02.

### Functional Localization of LGN

The locations of bilateral LGN were defined based on the visual stimulation experiment. The BOLD activation maps associated with the full-field visual stimulation were obtained through conventional general linear model (GLM) analysis as implemented in FSL. For each subject, the statistical parametric map (in terms of z-values) was normalized to the MNI space. Individual subjects' results were averaged and tested for group-level significance using one-sample t-test with $q<0.02$. The significantly activated voxels within the thalamus were considered to represent LGN instead of Pul, since passive viewing of visual

stimulation while maintaining fixation has been previously shown not to induce significant activation within Pul (Kastner et al., 2004).

### Anatomical Imaging of Thalamic Sub-divisions

For 10 of the subjects, high-resolution phase images were obtained from high-resolution multi-echo GRE data acquired under 7 T. The phase data for the first echo (TE=15.5 ms) were unwrapped using PRELUDE in FSL. Macroscopic phase distribution was removed from the unwrapped phase to yield phase images showing local susceptibility-weighted contrast. The unit of phase images was converted to frequency in Hz after divided by $2\pi$ and TE.

For comparison with functional images, the phase images were also normalized to the MNI space. This was achieved by first aligning the magnitude images at TE=30 ms to the $T_1$*-weighted images (using align_epi_anat.py in AFNI), which was in turn aligned to the MNI $T_1$*-weighted template (using FNIRT in FSL). The resulting transformational operations were sequentially applied to the phase images to allow for the alignment and averaging of individual subjects' phase images in the MNI space. The average phase images of these 10 subjects in the MNI space served as an MRI-based anatomical atlas of the thalamus for the entire 15 subjects' functional data set, offering much more structural detail than the conventional $T_1$-weighted MRI atlas, which appeared largely homogeneous in the thalamus. We used the phase images to address whether the thalamic regions functionally identified with alpha-BOLD correlation and visual activation analyses were structurally distinct.

### Comparison to Thalamic Atlas

In addition, we used the Morel atlas of the human thalamus (Morel, 2007) to confirm the structure-function relationship addressed with MRI and EEG as aforementioned, and to further relate fMRI-EEG findings to specifically named groups of thalamic nuclei. The Morel atlas is based on a comprehensive histological study of subcortical structures (Morel et al., 1997), and consists of named subgroups of nuclei with defined boundaries. We digitized 59 subgroups of nuclei on 26 drawings of horizontal sections of the thalamus, which were parallel to the intercommissural plane with an intersectional spacing of 0.9mm (Morel, 2007). We co-registered the digitized drawings to the MNI brain template by aligning their intercommissural planes and corresponding locations for the anterior and posterior commissure. As the atlas only included the right half of the thalamus, the left half was added to be symmetric to the right half. Such co-registered Morel atlas delineated ROIs in the MNI space for the 59 thalamic nuclei.

In order to comparatively attribute the negative alpha-BOLD correlations and visually evoked BOLD responses to specific subgroups of the visual thalamus, we performed receiver operating characteristic (ROC) analysis. This analysis was performed to separately characterize two functional maps (i.e. alpha-BOLD correlation map and visually evoked activation map), with either Pul or LGN serving as the "receiver" for each of these maps. The alpha-BOLD correlation map was subject to a negative statistical threshold, whereas the visual activation map was subject to a positive statistical threshold. For either case, the threshold used for the selection of voxels within the thalamus was varied stepwise. For each threshold chosen, we computed the true positive rate (TPR) as the number of selected thalamic voxels within the "receiver" divided by the total number of voxels in the "receiver". Note that the computation was based on voxels covering the entire thalamus. Similarly, we computed the false positive rate (FPR) as the number of selected thalamic voxels outside the "receiver" divided by the total number of thalamic voxels outside the "receiver". The TPR values found for the various thresholds were then plotted as a function of their corresponding FPR value, giving rise to an ROC curve. For a non-receiver specific

process, the ROC curve is an identity line. The better the "receiver" characterizes a process (i.e. a spatial distribution in this context), the higher the ROC curve runs above the identity line.

### Resting-State Functional Connectivity

From the group-level result of alpha-BOLD correlation (see RESULTS), two thalamic ROIs were defined for further functional connectivity analysis. The first ROI consisted of the lateral and posterior clusters of voxels showing significantly negative correlation with the posterior alpha; the second ROI was the anterior and medial dorsal region showing significantly positive correlation with the posterior alpha modulation. Both ROIs served separately as the seed ROI from which the functional connectivity to the rest of the brain was evaluated by computing the seeded cross correlation in the resting-state BOLD signal. This analysis was conducted in order to reveal the thalamocortical functional networks in which these two thalamic ROIs were individually involved.

## RESULTS

To find the hemodynamic correlates of posterior alpha EEG, we simultaneously measured EEG and fMRI signals from subjects resting with eyes closed. As the peak frequency in the alpha band varied across subjects, we first determined the individual alpha frequency (IAF) based on each subject's spectral contrast between the eyes-closed and eyes-open periods as shown in Fig. 1. The mean and standard deviation of IAF were 10.1 and 0.9 Hz, respectively. Linear correlation was evaluated between the spontaneous power fluctuation of the occipital EEG signal at the IAF and the BOLD-fMRI signal at every voxel in the brain. Fig. 2 shows the map of either positive or negative correlations that were statistically significant at the group level ($q<0.02$ for $n=15$). In cortex, only negative correlations were consistently found across subjects, being the strongest in the occipital lobe ($r=-0.21\pm0.04$, 4803 voxels for a $3\times3\times3$ $mm^3$ voxel size), and still significant but weaker in the parietal ($r=-0.16\pm0.04$, 4673 voxels), temporal ($r=-0.15\pm0.03$, 2071 voxels) and frontal ($r=-0.14\pm0.03$, 3914 voxels) lobes. These negatively correlated regions covered 55% of the visual cortex, including primary and higher visual areas distributed along both dorsal and ventral pathways. Some non-visual areas, such as the somatosensory and auditory cortices, also showed negative correlations. Interestingly, in the thalamus, we observed both negative and positive BOLD correlates to the posterior alpha power. The lateral and posterior parts of the left and right thalamus showed negative correlations ($r=-0.15\pm0.02$, 168 voxels), whereas the anterior and medial dorsal parts of the thalamus showed positive correlations ($r=0.19\pm0.02$, 154 voxels).

In light of previous animal electrophysiology studies (some of which mentioned in the Introduction section), we questioned whether such negatively correlated thalamic regions were within the visual thalamus. While the visual thalamus is known to include LGN and Pul, we first targeted the comparison with the LGN functionally localized with visual stimulation. Fig. 3 shows the group-level comparison between the BOLD activation with visual stimulation and the resting-state alpha-BOLD correlations. The bilateral LGN were clearly seen as two activation foci in the thalamus (Fig. 3.a). In contrast, the thalamic regions showing negative alpha-BOLD correlations were more extended, and appeared to be more medial and extend more dorsally (Fig. 3.b). Quantitatively, the thalamic regions showing significant negative alpha-BOLD correlations differed from the functionally localized LGN: it was four times larger and its peak correlation level was displaced by 7.5mm relative to the peak of LGN activity in the localizer; furthermore, only 17% of the region was overlapped by the LGN. This difference in location and extent led us to postulate that the negative alpha-BOLD correlations were not confined to LGN, but rather involved other thalamic structures.

To further compare the thalamic localization of stimulus-evoked activity and the BOLD-correlate of alpha activity during rest, we overlaid the respective functional maps on high-resolution GRE phase images (Fig. 4). Unlike $T_1$-weighted images, the $T_2$*-weighted phase images provided rich anatomical contrast among distinct thalamic sub-regions and surrounding tissues. The purpose of using the phase images was to test whether the negative alpha-BOLD correlations and the visually activated response occurred at different parts of the same nuclei or different nuclei, which should be indicated as homogeneous or inhomogeneous phase distribution. It was shown that the functionally localized LGN based on visual stimulation were located at the most lateral and inferior part of the posterior thalamus and close to the juncture of optic tract and radiation (Fig. 4a). The regions negatively correlated with alpha were more medial and showed positive frequency shift (i.e. lower intensity in the underlying phase images) (Fig. 4b), as opposed to negative frequency shift at the functionally localized LGN (Fig. 4a). These phase images indicated that there are anatomically distinct structures in the thalamus underlying these two functional regions. From these results, we further hypothesized that the thalamic structures showing the negative alpha-BOLD correlations localize to Pul.

To test this hypothesis, we also co-registered these functional maps with the so-called Morel atlas (Morel, 2007). As shown in Fig. 5a), the negative BOLD correlates to the posterior alpha power were mostly located within or close to Pul, whereas the BOLD responses induced by the visual stimulation were mostly confined to LGN. We also plotted the ROC curves for Pul (Fig. 5b) and LGN (Fig. 5c) with varying thresholds applied to the negative alpha-BOLD correlations (in blue) and the positive visual activations (in red) within the thalamus. Note that the ROC curve in blue runs above the red curve in Fig. 5b, but below the red curve in Fig. 5c. This result supports our hypothesis that negative alpha-BOLD correlation primarily localizes to Pul whereas visually evoked activity primarily localizes to LGN.

A thalamic region where the BOLD signal is correlated with the posterior alpha power may not contribute to the genesis of posterior alpha rhythms, unless this region is connected directly or indirectly to the cortical regions that actually generate alpha rhythms measurable with scalp EEG, which has very low sensitivity to thalamic sources. Therefore, we further evaluated thalamo-cortical functional connectivity with seed ROIs within regions that were correlated either negatively or positively with the posterior alpha power. We first defined a seed ROI including the left and right Pul, where significantly negative alpha-BOLD correlations were found. As can be seen from Fig. 6a), the cortical regions that were functionally connected to this Pul ROI largely coincided with the cortical regions that were negatively correlated with the posterior alpha power, showing 68% spatial overlap and −0.63 spatial correlation. Secondly, we chose a seed ROI in the anterior nuclei (AD) and medial dorsal nuclei (MDN), which were found to correlate significantly and positively with the posterior alpha power. This ROI was neither correlated nor anti-correlated with any of the cortical regions where we found BOLD correlates to the posterior alpha power. Instead, functional connectivity to this ROI involved anterior cingulate cortex, dorsal posterior cingulate cortex, cerebellum and brain stem. These functional connectivity patterns were also reproduced in an independent set of resting-state fMRI at 7T (see Figure S3 in the supplementary materials).

## DISCUSSION

Using simultaneous EEG-fMRI, we found both negative and positive correlations between the fMRI signals from the thalamus and the spontaneous modulation of posterior alpha rhythms. The negative correlations were mostly seen within the visual thalamus, with a preference for the pulvinar over LGN. Based on the analysis of correlations within the fMRI

data, these regions appeared to form widespread functional connections with cortical regions in the visual cortex and beyond, where fMRI signals were negatively correlated with posterior alpha modulation. Positive correlations between posterior alpha and fMRI signals were constrained to the anterior and medial dorsal nuclei of the thalamus. Interestingly, and in contrast with the findings for the pulvinar, fMRI signals in these regions appeared dissociated (i.e. neither correlated nor anti-correlated) from signals in the visual cortex. Rather, they were functionally connected with a distinct network that included anterior and posterior cingulate cortex, cerebellum and brain stem.

## Thalamic Mechanisms of Posterior Alpha Rhythm

Where does the posterior alpha rhythm originate in the human brain? It is widely understood that alpha rhythms measurable with scalp EEG, or magnetoencephalography (MEG), arise from the cortex. EEG/MEG sensors are strongly biased for electrical activity from the cortex compared to the thalamus. Perhaps for this reason, noninvasive imaging based on EEG/MEG has only revealed extended areas in the occipital and parietal cortex, but not in the thalamus, as the generators of alpha rhythmic activity (Mitra and Bokil, 2008). However, this sensitivity bias does not preclude the thalamus from contributing to cortical alpha rhythms. Indeed, the thalamus has been proposed to play an active role in generating and modulating alpha rhythmic activity. An appealing proposal is that a thalamic “pacemaker” initiates cortical alpha rhythms (Andersen and Andersson, 1968). This thalamic pacemaker is thought to consist of inhibitory neurons firing at roughly 10Hz during wakeful rest. The rhythmic spiking activity causes inhibitory postsynaptic potentials of thalamocortical neurons to oscillate at the alpha frequency. This oscillation can be further passed onto the cortex through thalamocortical connections. In contrast, another plausible thalamic mechanism of alpha rhythms put more emphasis on the reciprocal interaction between the thalamus and the cortex, as opposed to considering the cortex merely as a passive recipient of alpha rhythms (Hughes and Crunelli, 2005). In this mechanism, a subset of thalamocortical neurons, called high-threshold bursting neurons, initiate thalamic alpha rhythms at other thalamocortical neurons with the presence of modulatory corticothalamic feedback. In turn, thalamic alpha rhythms are transmitted to the cortex through thalamocortical feedforward inputs. Despite the difference between the two mechanisms, they both imply synchronized and co-modulated alpha rhythms at thalamocortical neurons and their projecting cortical regions. In other words, their alpha oscillations should exhibit a consistent phase relationship (i.e. synchronization); the amplitude modulations of their alpha oscillations should be correlated in time (i.e. co-modulation).

## Negative Correlation between alpha-EEG and Thalamic BOLD-fMRI

While increasing evidence from animal electrophysiology has strongly supported a joint involvement of thalamus and cortex in the generation of the alpha rhythm (Chatila et al., 1992; Chatila et al., 1993; Hughes and Crunelli, 2005; Lopes da Silva et al., 1973; Lopes da Silva et al., 1980), evidence obtained from humans is lacking. Since electrophysiological signals within the thalamus are not noninvasively accessible for humans, it is very difficult to directly verify the synchronization and co-modulation of alpha rhythms between the corresponding parts of the thalamus and the cortex. However, one may use simultaneous EEG-fMRI to indirectly assess the co-modulation of alpha rhythms, assuming that the modulation of regional alpha rhythm has a similar regional hemodynamic effect for both the cortex and the thalamus. Under this assumption, coherence of alpha modulation between thalamic and cortical regions predicts that the BOLD-fMRI signals at these regions are also correlated, in a similar fashion, with the cortical alpha power measured with EEG. It is worth noting that concurrent EEG-fMRI cannot be used to verify the phase synchrony of alpha rhythms between two regions, simply because the alpha oscillation itself is too fast to be detected by fMRI.

As far as the posterior alpha is concerned, its cortical sources are thought to arise primarily from regions processing visual information. This is especially the case for occipital and parietal alpha signals, as has been consistently observed in EEG/MEG source localization studies (Michel et al., 1992; Mitra and Bokil, 2008; Yang et al., 2010). In those cortical areas, we report negative correlations between the BOLD signal and the posterior alpha power, as also shown in most other EEG-fMRI studies following a similar rationale (de Munck et al., 2007; Feige et al., 2005; Goldman et al., 2002; Moosmann et al., 2003; Sadaghiani et al., 2010). A novel finding of the present study is that the negative thalamic BOLD-correlate of posterior alpha power localizes to the visual thalamus. This finding contributes to bridging the gap between the interpretation of human imaging data and animal electrophysiology data, and provides indirect evidence supporting the hypothesis that there are coherent modulations of alpha rhythms between the thalamic and cortical parts of the human visual system. In addition, we found functional connectivity between the visual thalamus and the visual cortex in agreement with their previously established anatomical connection.

### Pul vs. LGN

When attempting to describe the relationship of the thalamus with posterior alpha modulation, it is important to consider its functional and structural heterogeneity. In fact, even the visual part of the thalamus includes different subgroups of nuclei (e.g. Pul and LGN) that serve distinct functions (Saalmann and Kastner, 2011) and appear differently in anatomy (Jones, 2007; Morel, 2007). Conventionally, LGN is considered a first-order thalamic nucleus and serves primarily as a relay station that transmits retinal inputs to primary visual cortex (V1) with no or relatively sparse projections to other visual areas. Pul, as the largest nucleus in the human thalamus, is considered a higher-order thalamic nucleus. Unlike LGN, Pul is extensively connected to the entire visual cortex, including its ventral and dorsal pathways (Kaas and Lyon, 2007). Although the precise functions of Pul remain poorly understood, increasing evidence suggests that it may play a modulatory role in cortico-cortical information transfer via trans-pulvinar pathways (Sherman and Guillery, 2011).

Interestingly, we found that Pul, rather than LGN, is more likely associated with the spontaneous modulation of posterior alpha rhythm. To find out where the negative alpha-BOLD correlations occurred in the thalamus, we sequentially used the following three steps that involved three independent data sets as reference for comparison. First, we compared with functionally localized LGN based on the same imaging sequence and preprocessing. This comparison showed that negative alpha-BOLD correlations occurred near LGN but not at LGN, appearing more medial and dorsal with larger extent (Fig. 3). Second, we compared with in vivo GRE phase images to show that negative alpha-BOLD correlated regions and functionally localized LGN were structurally distinct, suggesting that they occurred at different thalamic nuclei instead of different parts of the same nuclei (Fig. 4). Third, we finally compared with the histology-based atlas to identify the nuclei: the negative alpha-BOLD correlations localize to Pul; the visual activation localize to LGN, which was confirmative and as expected (Fig. 5). These three sets of data offered complementary information about the function-structure relationship, while being mutually supportive and collectively leading to our conclusion.

Consistent with our finding, Lopes da Silva et al. also found a much larger and widespread influence of Pul on cortical alpha synchronization in dogs' brain (Lopes da Silva et al., 1980). For the human brain, Lukashevich and Sazonova reported that lesions in the posterior thalamus resulted in the alpha-rhythm suppression up to its total elimination for a number of patients (Lukashevich and Sazonova, 1996). However, recent animal electrophysiology studies have primarily targeted LGN for studying thalamic alpha signals (Lorincz et al.,

2009) while data on Pul remain sparse. It is also interesting to note that Pul and posterior alpha rhythm share a common evolutionary trend for mammals. Animals showing alpha equivalent activity, such as primates, dogs and cats, all have Pul in their visual system, whereas Pul does not seem to exist in brains of rodents, whose visual system also show little alpha activity (Hughes and Crunelli, 2005; Pessoa and Adolphs, 2010). In addition, the extensive functional (as shown in Fig. 5a) and anatomical (Shipp, 2003) connections between Pul and the cortex make Pul well suitable to behave as a thalamic control unit for the widespread cortical alpha activity.

A plausible linkage between Pul and alpha rhythm is also conceivable in light of their similar functional association with the control of visual attention. Previous fMRI studies have shown that covert attention to visual stimuli lead to activation (Kastner et al., 2004), or enhancement of activation (Smith et al., 2009), in Pul. Lesion or inactivation to Pul was also found to result in impaired attentional selection (Snow et al., 2009) or movement planning (Wilke et al., 2010). Along an independent line of research, the posterior alpha rhythm has been reported to be a marker of visual attention (Foxe et al., 1998; Kelly et al., 2006; Sauseng et al., 2005; Thut et al., 2006) and be able to influence behavioral and perceptual performance (Sauseng et al., 2005; van Dijk et al., 2008). However, Pul and alpha rhythms have rarely been examined together in relation to visual attention or brain functions in general (Wilke et al., 2009). For this reason, we would argue that Pul may be an important target for future studies pertaining to alpha rhythms as well as other related cortical states and functions. Concurrent EEG-fMRI would be an ideal methodological choice for this research direction.

### Positive Correlation between alpha-EEG and Thalamic BOLD-fMRI

Some previous EEG-fMRI/PET studies have reported positive correlations between BOLD signals in the thalamus and the posterior alpha EEG, and have often interpreted this finding as evidence in support of the thalamic pacemaker for alpha (Danos et al., 2001; de Munck et al., 2007; Feige et al., 2005; Goldman et al., 2002; Moosmann et al., 2003; Sadaghiani et al., 2010; Sadato et al., 1998). In the present study, we confirmed this finding and further pinpointed such positive correlations specifically to anterior and medial dorsal nuclei. However, interpreting this result as supporting evidence of the thalamic pacemaker mechanism may be questionable for the following reasons. First, anterior and medial dorsal nuclei are not known to consist of inhibitory neurons, which would be anticipated if they would serve as pacemaker cells. Secondly, the pacemaker cells should be connected, either directly or indirectly through LGN and/or Pul, to the visual cortex, which shows strong alpha activity. Here, we tested the second point by evaluating resting-state functional connectivity from the fMRI data. Our results (Fig. 5b) show no evidence of functional connectivity between the anterior and medial dorsal nuclei and the visual cortex. Instead, these thalamic nuclei appear functionally connected to the anterior cingulate cortex, dorsal posterior cingulate cortex, brain stem and cerebellum. This network has been known to mediate a variety of brain functions, such as cortical arousal (Saper et al., 2005; Steriade, 1996), emotional processing (Metzger et al., 2010) and tonic alertness (Sadaghiani et al., 2010). Therefore, our finding calls for caution with simply interpreting positive alpha-BOLD correlation as evidence for the hypothesis that alpha rhythms originate from a thalamic “pacemaker”.

However, we do not rule out the possibility that activity at anterior and medial dorsal nuclei may take part in a modulatory control, related to vigilance or arousal, which also influences cortical alpha rhythms (Olbrich et al., 2009). Indeed, the location of thalamic nuclei with positive BOLD-alpha correlation overlap with that of the ascending reticular activating system (ARAS) (Moruzzi and Magoun, 1949), and in particular its cholinergic component (Shute and Lewis, 1967). This ascending component also serves as a part of a larger

cholinergic limbic system that includes cingulate cortex and is able to profoundly affect cortical activity (Lewis and Shute, 1967), behavior and emotion (Bush et al., 2000). In addition, the ascending modulatory system also sends inputs to other thalamic relay nuclei (e.g. Pul) as well as reticular nuclei, which has been suggested to play an important role in regulating thalamocortical oscillation and transmission in the sleeping and aroused brain (Steriade et al., 1993). Therefore, we speculate that while the pulvinar may be intimately involved in the generation of the alpha rhythm in the occipital cortex, such rhythmic activities may be under central modulatory control (Steriade, 1993) effectuated through the midline and anterior parts of the thalamus (Saper et al., 2005).

### Limitations

Since the thalamus is known to contain distinct nuclei closely packed within a relatively small volume, it would be preferable to use higher spatial resolution than used in this study for optimal distinction between different functional subgroups of the thalamus. However compared to the cortex, the thalamus is a more challenging target for fMRI due to its deeper location and longer distance from the receive coil array. This physically limits the sensitivity (quantified by the signal to noise ratio, or SNR) inside the thalamus. SNR is further reduced when increasing the spatial resolution, as it is inversely proportional to voxel volume. Moreover, simultaneous EEG-fMRI places additional technical constraints. The higher spatial resolution requires longer time for each slice acquisition, which in turn results in a higher level of gradient artifacts EEG, While fMRI sensitivity could be improved by scanning at higher field strength, currently no commercial EEG systems are approved for use at higher field strength due to safety concerns. In light of these considerations, we used relatively low spatial resolution (3.4 mm in-plane resolution with 4 mm slice thickness) for the 15 subjects reported in this paper. To explore potential benefits of higher resolution, we repeated the experiments described above with 3 mm and 2 mm isotropic voxels on a single subject on a 3 T scanner (Skyra, Siemens, Germany) using a 64-channel EEG system. We were able to reproduce our previous finding with 3 mm resolution, showing that negative correlates to posterior alpha power and positive responses to visual stimulation occurred at different thalamic subregions with little spatial overlap (Figure S1). At 2 mm resolution, the sensitivity to thalamic signals was too low to reliably reveal either LGN or Pul based on visual activation or alpha correlation (Figure S2).

Although the present study contributes to finding the thalamic substrates involved in the alpha modulation, it does not answer why such a modulation occurs spontaneously or what its functional significance is. The modulation of alpha rhythms may in part be associated with fluctuations in the arousal level or cognitive load. Another outstanding question is whether the fMRI correlate and role of alpha differ between sleep states, for example between rapid eye movement (REM) sleep and wakefulness, which show similar EEG signals. The distinction between these two conditions in terms of alpha modulation mechanism remains to be addressed in the future.

## CONCLUSION

Analysis of EEG-fMRI and fMRI-fMRI correlation patterns in human resting state data suggests that the pulvinar nucleus in the thalamus is intimately involved in the generation and spontaneous modulation of posterior alpha rhythms, consistent with its reciprocal and widespread anatomical connectivity to cortical visual areas. In contrast, the anterior and medial dorsal nuclei, as part of the ascending neuromodulatory system, may indirectly modulate cortical alpha rhythms as a way to modulate vigilance and arousal levels, or as a result thereof.

## Supplementary Material

Refer to Web version on PubMed Central for supplementary material.

## References


Andersen, P.; Andersson, S. Physiological basis of the alpha rhythm. Appleton-Century-Crofts; New York: 1968.

Behrens TE, Johansen-Berg H, Woolrich MW, Smith SM, Wheeler-Kingshott CA, Boulby PA, Barker GJ, Sillery EL, Sheehan K, Ciccarelli O, Thompson AJ, Brady JM, Matthews PM. Non-invasive mapping of connections between human thalamus and cortex using diffusion imaging. Nat Neurosci. 2003; 6:750–757. [PubMed: 12808459]

Berger H. Über das Elektrenkephalogramm des Menschen. Arch Psychiatr Nervenkr. 1929; 87:527–570.

Birn RM, Smith MA, Jones TB, Bandettini PA. The respiration response function: the temporal dynamics of fMRI signal fluctuations related to changes in respiration. Neuroimage. 2008; 40:644–654. [PubMed: 18234517]

Buchsbaum MS, Kessler R, King A, Johnson J, Cappelletti J. Simultaneous cerebral glucography with positron emission tomography and topographic electroencephalography. Prog Brain Res. 1984; 62:263–269. [PubMed: 6335920]

Bush G, Luu P, Posner MI. Cognitive and emotional influences in anterior cingulate cortex. Trends Cogn Sci. 2000; 4:215–222. [PubMed: 10827444]

Chang C, Cunningham JP, Glover GH. Influence of heart rate on the BOLD signal: the cardiac response function. Neuroimage. 2009; 44:857–869. [PubMed: 18951982]

Chatila M, Milleret C, Buser P, Rougeul A. A 10 Hz “alpha-like” rhythm in the visual cortex of the waking cat. Electroencephalogr Clin Neurophysiol. 1992; 83:217–222. [PubMed: 1381673]

Chatila M, Milleret C, Rougeul A, Buser P. Alpha rhythm in the cat thalamus. C R Acad Sci III. 1993; 316:51–58. [PubMed: 8495387]

Cox RW. AFNI: software for analysis and visualization of functional magnetic resonance neuroimages. Comput Biomed Res. 1996; 29:162–173. [PubMed: 8812068]

Danos P, Guich S, Abel L, Buchsbaum MS. EEG alpha rhythm and glucose metabolic rate in the thalamus in schizophrenia. Neuropsychobiology. 2001; 43:265–272. [PubMed: 11340367]

de Munck JC, Goncalves SI, Huijboom L, Kuijer JP, Pouwels PJ, Heethaar RM, Lopes da Silva FH. The hemodynamic response of the alpha rhythm: an EEG/fMRI study. Neuroimage. 2007; 35:1142–1151. [PubMed: 17336548]

de Zwart JA, van Gelderen P, Kellman P, Duyn JH. Application of sensitivity-encoded echo-planar imaging for blood oxygen level-dependent functional brain imaging. Magn Reson Med. 2002; 48:1011–1020. [PubMed: 12465111]

Duyn JH, van Gelderen P, Li TQ, de Zwart JA, Koretsky AP, Fukunaga M. High-field MRI of brain cortical substructure based on signal phase. Proc Natl Acad Sci U S A. 2007; 104:11796–11801. [PubMed: 17586684]

Elias WJ, Zheng ZA, Domer P, Quigg M, Pouratian N. Validation of connectivity-based thalamic segmentation with direct electrophysiologic recordings from human sensory thalamus. Neuroimage. 2012; 59:2025–2034. [PubMed: 22036683]

Feige B, Scheffler K, Esposito F, Di Salle F, Hennig J, Seifritz E. Cortical and subcortical correlates of electroencephalographic alpha rhythm modulation. J Neurophysiol. 2005; 93:2864–2872. [PubMed: 15601739]

Foxe JJ, Simpson GV, Ahlfors SP. Parieto-occipital approximately 10 Hz activity reflects anticipatory state of visual attention mechanisms. Neuroreport. 1998; 9:3929–3933. [PubMed: 9875731]

Glover GH, Li TQ, Ress D. Image-based method for retrospective correction of physiological motion effects in fMRI: RETROICOR. Magn Reson Med. 2000; 44:162–167. [PubMed: 10893535]

Goldman RI, Stern JM, Engel J Jr, Cohen MS. Simultaneous EEG and fMRI of the alpha rhythm. Neuroreport. 2002; 13:2487–2492. [PubMed: 12499854]

Hughes SW, Crunelli V. Thalamic mechanisms of EEG alpha rhythms and their pathological implications. Neuroscientist. 2005; 11:357–372. [PubMed: 16061522]

Johansen-Berg H, Behrens TE, Sillery E, Ciccarelli O, Thompson AJ, Smith SM, Matthews PM. Functional-anatomical validation and individual variation of diffusion tractography-based segmentation of the human thalamus. Cereb Cortex. 2005; 15:31–39. [PubMed: 15238447]

Jones, EG. The Thalamus. Cambridge University Press; New York, USA: 2007.

Kaas JH, Lyon DC. Pulvinar contributions to the dorsal and ventral streams of visual processing in primates. Brain Res Rev. 2007; 55:285–296. [PubMed: 17433837]

Kastner S, O'Connor DH, Fukui MM, Fehd HM, Herwig U, Pinsk MA. Functional imaging of the human lateral geniculate nucleus and pulvinar. J Neurophysiol. 2004; 91:438–448. [PubMed: 13679404]

Kelly SP, Lalor EC, Reilly RB, Foxe JJ. Increases in alpha oscillatory power reflect an active retinotopic mechanism for distracter suppression during sustained visuospatial attention. J Neurophysiol. 2006; 95:3844–3851. [PubMed: 16571739]

Larson CL, Davidson RJ, Abercrombie HC, Ward RT, Schaefer SM, Jackson DC, Holden JE, Perlman SB. Relations between PET-derived measures of thalamic glucose metabolism and EEG alpha power. Psychophysiology. 1998; 35:162–169. [PubMed: 9529942]

Laufs H, Kleinschmidt A, Beyerle A, Eger E, Salek-Haddadi A, Preibisch C, Krakow K. EEG-correlated fMRI of human alpha activity. Neuroimage. 2003; 19:1463–1476. [PubMed: 12948703]

Lewis PR, Shute CC. The cholinergic limbic system: projections to hippocampal formation, medial cortex, nuclei of the ascending cholinergic reticular system, and the subfornical organ and supra-optic crest. Brain. 1967; 90:521–540. [PubMed: 6058141]

Lindgren KA, Larson CL, Schaefer SM, Abercrombie HC, Ward RT, Oakes TR, Holden JE, Perlman SB, Benca RM, Davidson RJ. Thalamic metabolic rate predicts EEG alpha power in healthy control subjects but not in depressed patients. Biol Psychiatry. 1999; 45:943–952. [PubMed: 10386175]

Liu Z, de Zwart JA, van Gelderen P, Kuo LW, Duyn JH. Statistical feature extraction for artifact removal from concurrent fMRI-EEG recordings. Neuroimage. 2012; 59:2073–2087. [PubMed: 22036675]

Lopes da Silva FH, van Lierop TH, Schrijer CF, van Leeuwen WS. Organization of thalamic and cortical alpha rhythms: spectra and coherences. Electroencephalogr Clin Neurophysiol. 1973; 35:627–639. [PubMed: 4128158]

Lopes da Silva FH, Vos JE, Mooibroek J, Van Rotterdam A. Relative contributions of intracortical and thalamo-cortical processes in the generation of alpha rhythms, revealed by partial coherence analysis. Electroencephalogr Clin Neurophysiol. 1980; 50:449–456. [PubMed: 6160987]

Lorincz ML, Kekesi KA, Juhasz G, Crunelli V, Hughes SW. Temporal framing of thalamic relay-mode firing by phasic inhibition during the alpha rhythm. Neuron. 2009; 63:683–696. [PubMed: 19755110]

Lukashevich IP, Sazonova OB. The effect of lesions of different parts of the optic thalamus on the nature of the bioelectrical activity of the human brain. Zh Vyssh Nerv Deiat Im I P Pavlova. 1996; 46:866–874. [PubMed: 9054138]

Metzger CD, Eckert U, Steiner J, Sartorius A, Buchmann JE, Stadler J, Tempelmann C, Speck O, Bogerts B, Abler B, Walter M. High field FMRI reveals thalamocortical integration of segregated cognitive and emotional processing in mediodorsal and intralaminar thalamic nuclei. Front Neuroanat. 2010; 4:138. [PubMed: 21088699]

Michel CM, Lehmann D, Henggeler B, Brandeis D. Localization of the sources of EEG delta, theta, alpha and beta frequency bands using the FFT dipole approximation. Electroencephalogr Clin Neurophysiol. 1992; 82:38–44. [PubMed: 1370142]

Mitra, P.; Bokil, H. Observed Brain Dynamics. Oxford Univ. Press; 2008.

Moosmann M, Ritter P, Krastel I, Brink A, Thees S, Blankenburg F, Taskin B, Obrig H, Villringer A. Correlates of alpha rhythm in functional magnetic resonance imaging and near infrared spectroscopy. Neuroimage. 2003; 20:145–158. [PubMed: 14527577]

Morel, A. Stereotactic atlas of the human thalamus and basal ganglia. Informa Healthcare; USA, New York: 2007.

Morel A, Magnin M, Jeanmonod D. Multiarchitectonic and stereotactic atlas of the human thalamus. J Comp Neurol. 1997; 387:588–630. [PubMed: 9373015]

Moruzzi G, Magoun HW. Brain stem reticular formation and activation of the EEG. Electroencephalogr Clin Neurophysiol. 1949; 1:455–473. [PubMed: 18421835]

Niedermeyer E. Alpha rhythms as physiological and abnormal phenomena. Int J Psychophysiol. 1997; 26:31–49. [PubMed: 9202993]

Olbrich S, Mulert C, Karch S, Trenner M, Leicht G, Pogarell O, Hegerl U. EEG-vigilance and BOLD effect during simultaneous EEG/fMRI measurement. Neuroimage. 2009; 45:319–332. [PubMed: 19110062]

Pessoa L, Adolphs R. Emotion processing and the amygdala: from a 'low road' to 'many roads' of evaluating biological significance. Nat Rev Neurosci. 2010; 11:773–783. [PubMed: 20959860]

Saad ZS, Glen DR, Chen G, Beauchamp MS, Desai R, Cox RW. A new method for improving functional-to-structural MRI alignment using local Pearson correlation. Neuroimage. 2009; 44:839–848. [PubMed: 18976717]

Saalmann YB, Kastner S. Cognitive and perceptual functions of the visual thalamus. Neuron. 2011; 71:209–223. [PubMed: 21791281]

Sadaghiani S, Scheeringa R, Lehongre K, Morillon B, Giraud AL, Kleinschmidt A. Intrinsic connectivity networks, alpha oscillations, and tonic alertness: a simultaneous electroencephalography/functional magnetic resonance imaging study. J Neurosci. 2010; 30:10243–10250. [PubMed: 20668207]

Sadato N, Nakamura S, Oohashi T, Nishina E, Fuwamoto Y, Waki A, Yonekura Y. Neural networks for generation and suppression of alpha rhythm: a PET study. Neuroreport. 1998; 9:893–897. [PubMed: 9579686]

Saper CB, Scammell TE, Lu J. Hypothalamic regulation of sleep and circadian rhythms. Nature. 2005; 437:1257–1263. [PubMed: 16251950]

Sauseng P, Klimesch W, Stadler W, Schabus M, Doppelmayr M, Hanslmayr S, Gruber WR, Birbaumer N. A shift of visual spatial attention is selectively associated with human EEG alpha activity. Eur J Neurosci. 2005; 22:2917–2926. [PubMed: 16324126]

Sherman, SM.; Guillery, RW. Exploring the thalamus and its role in cortical function. MIT Press; Cambridge, MA: 2006.

Sherman SM, Guillery RW. Distinct functions for direct and transthalamic corticocortical connections. J Neurophysiol. 2011; 106:1068–1077. [PubMed: 21676936]

Shipp S. The functional logic of cortico-pulvinar connections. Philos Trans R Soc Lond B Biol Sci. 2003; 358:1605–1624. [PubMed: 14561322]

Shute CC, Lewis PR. The ascending cholinergic reticular system: neocortical, olfactory and subcortical projections. Brain. 1967; 90:497–520. [PubMed: 6058140]

Smith AT, Cotton PL, Bruno A, Moutsiana C. Dissociating vision and visual attention in the human pulvinar. J Neurophysiol. 2009; 101:917–925. [PubMed: 19073806]

Smith SM, Jenkinson M, Woolrich MW, Beckmann CF, Behrens TE, Johansen-Berg H, Bannister PR, De Luca M, Drobnjak I, Flitney DE, Niazy RK, Saunders J, Vickers J, Zhang Y, De Stefano N, Brady JM, Matthews PM. Advances in functional and structural MR image analysis and implementation as FSL. Neuroimage. 2004; 23(Suppl 1):S208–219. [PubMed: 15501092]

Snow JC, Allen HA, Rafal RD, Humphreys GW. Impaired attentional selection following lesions to human pulvinar: evidence for homology between human and monkey. Proc Natl Acad Sci U S A. 2009; 106:4054–4059. [PubMed: 19237580]

Steriade M. Central core modulation of spontaneous oscillations and sensory transmission in thalamocortical systems. Curr Opin Neurobiol. 1993; 3:619–625. [PubMed: 8219730]

Steriade M. Arousal: revisiting the reticular activating system. Science. 1996; 272:225–226. [PubMed: 8602506]

Steriade M, McCormick DA, Sejnowski TJ. Thalamocortical oscillations in the sleeping and aroused brain. Science. 1993; 262:679–685. [PubMed: 8235588]

Thut G, Nietzel A, Brandt SA, Pascual-Leone A. Alpha-band electroencephalographic activity over occipital cortex indexes visuospatial attention bias and predicts visual target detection. J Neurosci. 2006; 26:9494–9502. [PubMed: 16971533]

van Dijk H, Schoffelen JM, Oostenveld R, Jensen O. Prestimulus oscillatory activity in the alpha band predicts visual discrimination ability. J Neurosci. 2008; 28:1816–1823. [PubMed: 18287498]

Wilke M, Mueller KM, Leopold DA. Neural activity in the visual thalamus reflects perceptual suppression. Proc Natl Acad Sci U S A. 2009; 106:9465–9470. [PubMed: 19458249]

Wilke M, Turchi J, Smith K, Mishkin M, Leopold DA. Pulvinar inactivation disrupts selection of movement plans. J Neurosci. 2010; 30:8650–8659. [PubMed: 20573910]

Yang L, Liu Z, He B. EEG-fMRI reciprocal functional neuroimaging. Clin Neurophysiol. 2010; 121:1240–1250. [PubMed: 20378397]

Zhang D, Snyder AZ, Fox MD, Sansbury MW, Shimony JS, Raichle ME. Intrinsic functional relations between human cerebral cortex and thalamus. J Neurophysiol. 2008; 100:1740–1748. [PubMed: 18701759]

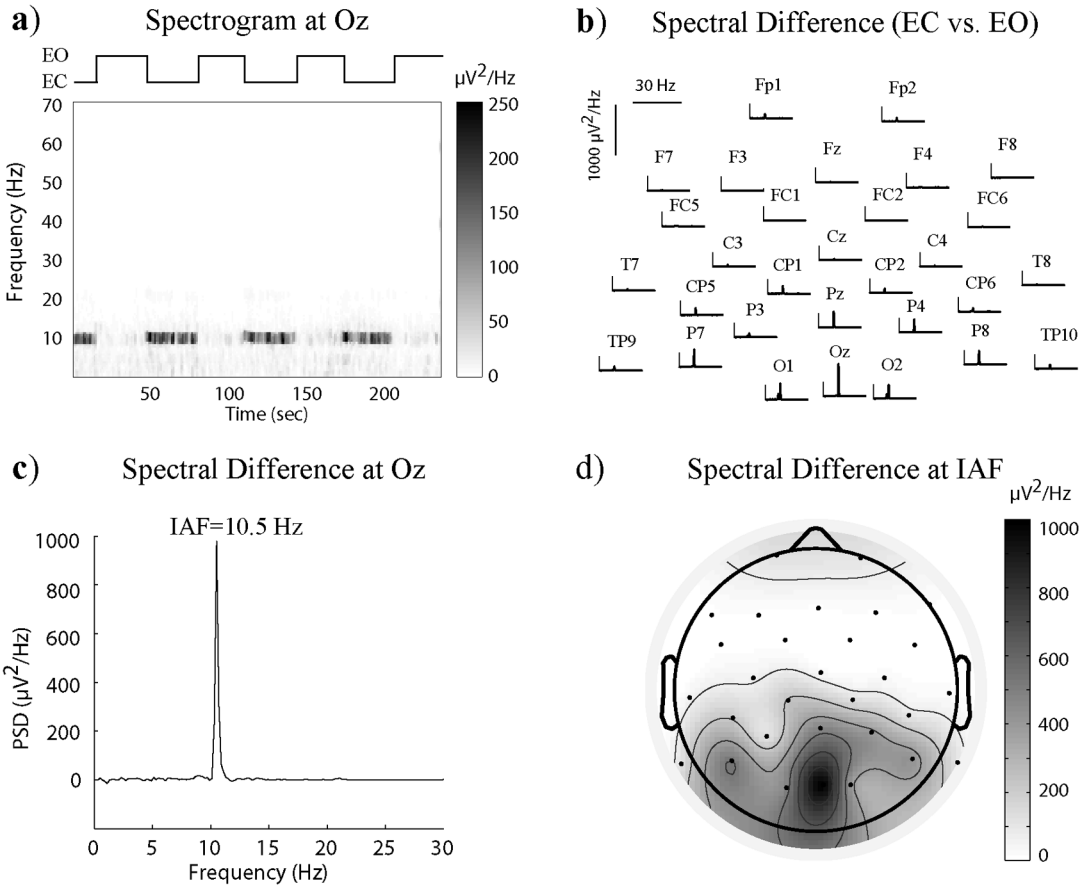


**Figure 1.**

Single-subject spectral contrast between eyes-closed and eyes-open periods. a) Spectrogram for the Oz channel during the voluntary eyes-close-eyes-open task; b) Spectral difference between the eyes-closed and eyes-open periods for all EEG channels; c) Spectral difference for the Oz channel with the IAF determined from the peak; d) The spatial distribution of the spectral difference specifically at the IAF.

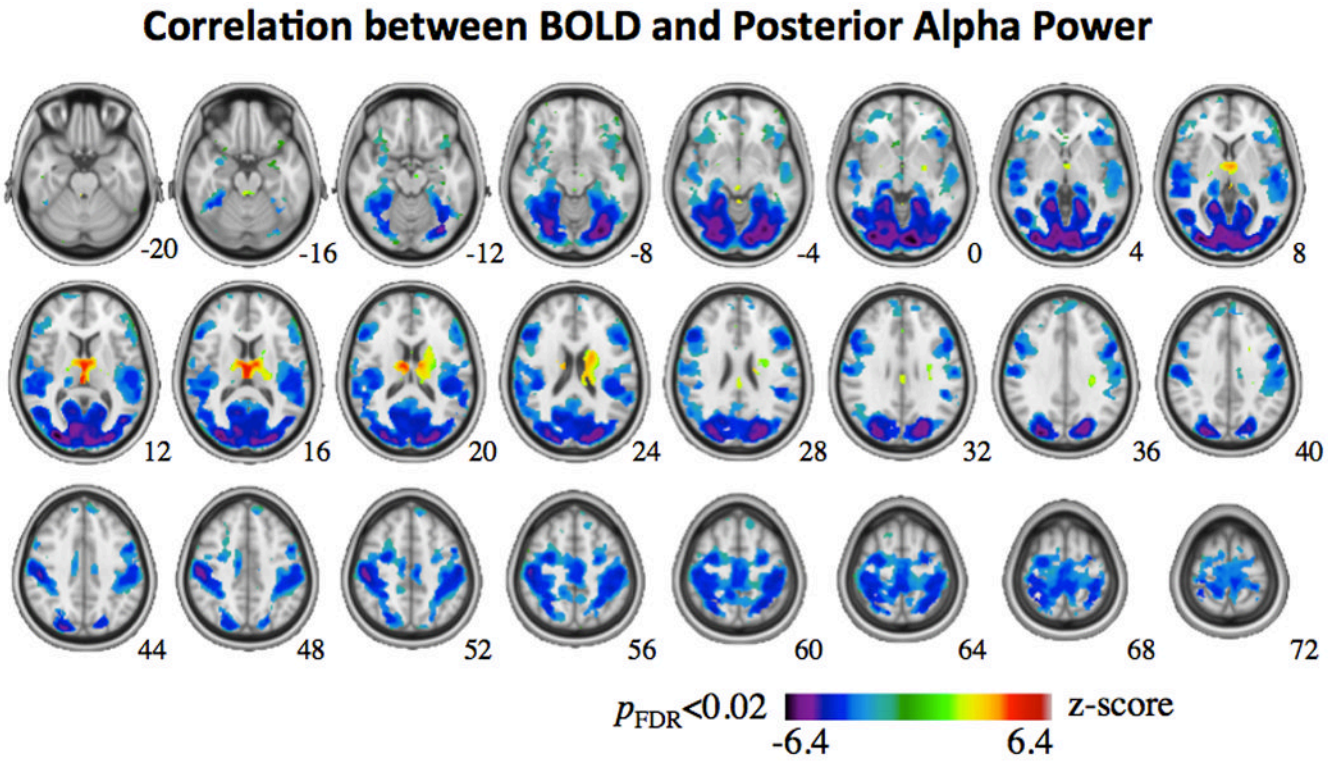


**Figure 2.**

Group-level map of BOLD correlates to posterior alpha power. The map shows the distribution of the mean voxel-wise correlation (represented in z score) averaged across 15 subjects, thresholded by a t-value that yields p<0.02 (corrected for FDR). The MNI z coordinate is shown in the left-bottom corner of each slice.

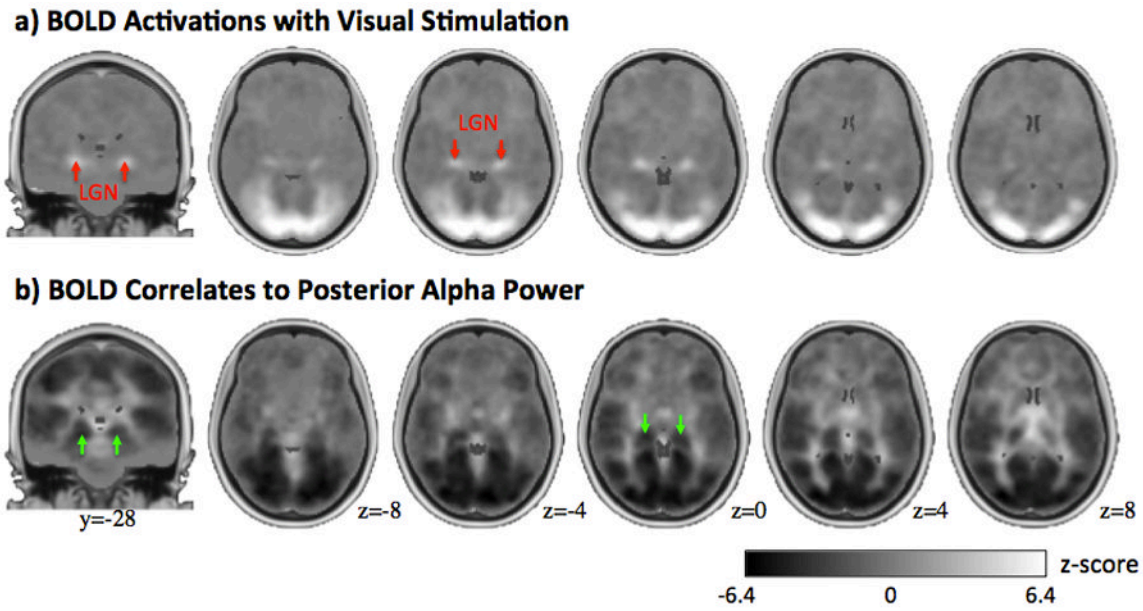


**Figure 3.**

Comparison between BOLD activations with visual stimulation (a) and BOLD correlates to posterior alpha power (b). Both maps are not thresholded. Two peak activations in the thalamus are indicated by the red arrows as LGN in a), or by the green arrows in b). The gray bar and MNI slice positions indicated in b) also applies to a).

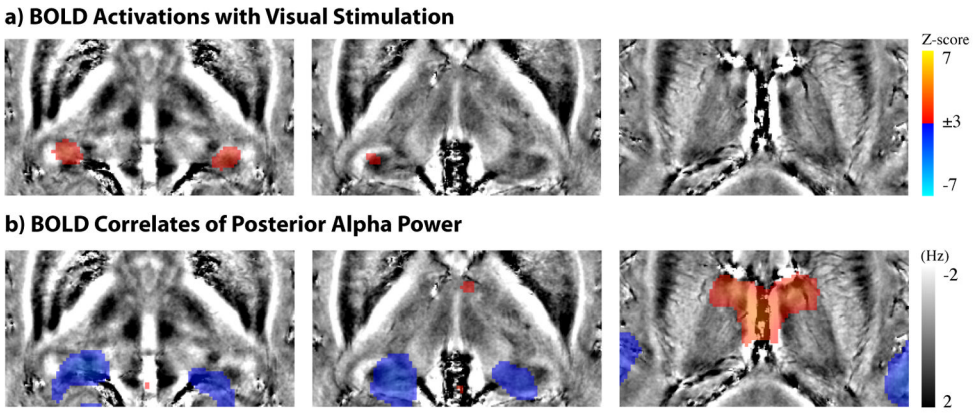


**Figure 4.**

Comparison between BOLD activations with visual stimulation (a) and BOLD correlates to posterior alpha power (b) with the underlay of high-resolution GRE phase images. The gray and color bars apply to the underlay and overlay, respectively for both a) and b). The three slices (from left to right) shown in both a) and b) are at z=−2, 2 and 13mm in MNI space.

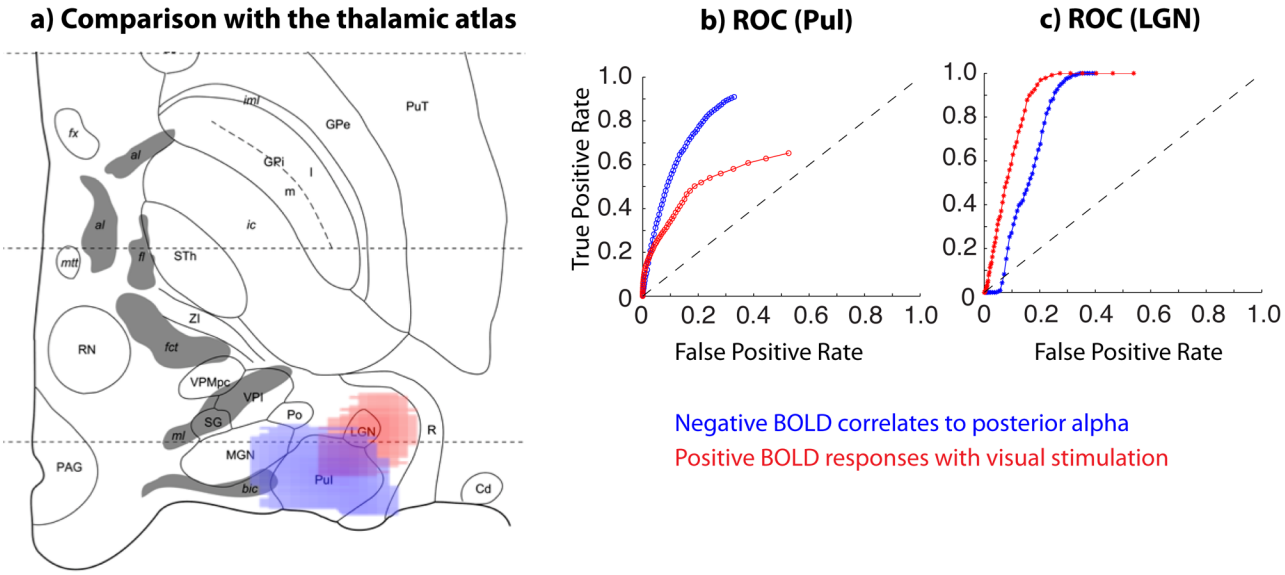


**Figure 5.**

a) BOLD activations with visual stimulation (red) and negative BOLD correlates to posterior alpha power (blue) overlaid on top of the histologically defined atlas of the thalamus, for a horizontal slice parallel to and 2.7mm below the intercommissural plane. The activation and correlation are thresholded with $p<0.02$ (corrected for FDR). b) ROC curves with respect to Pul, c) ROC curves with respect to LGN.

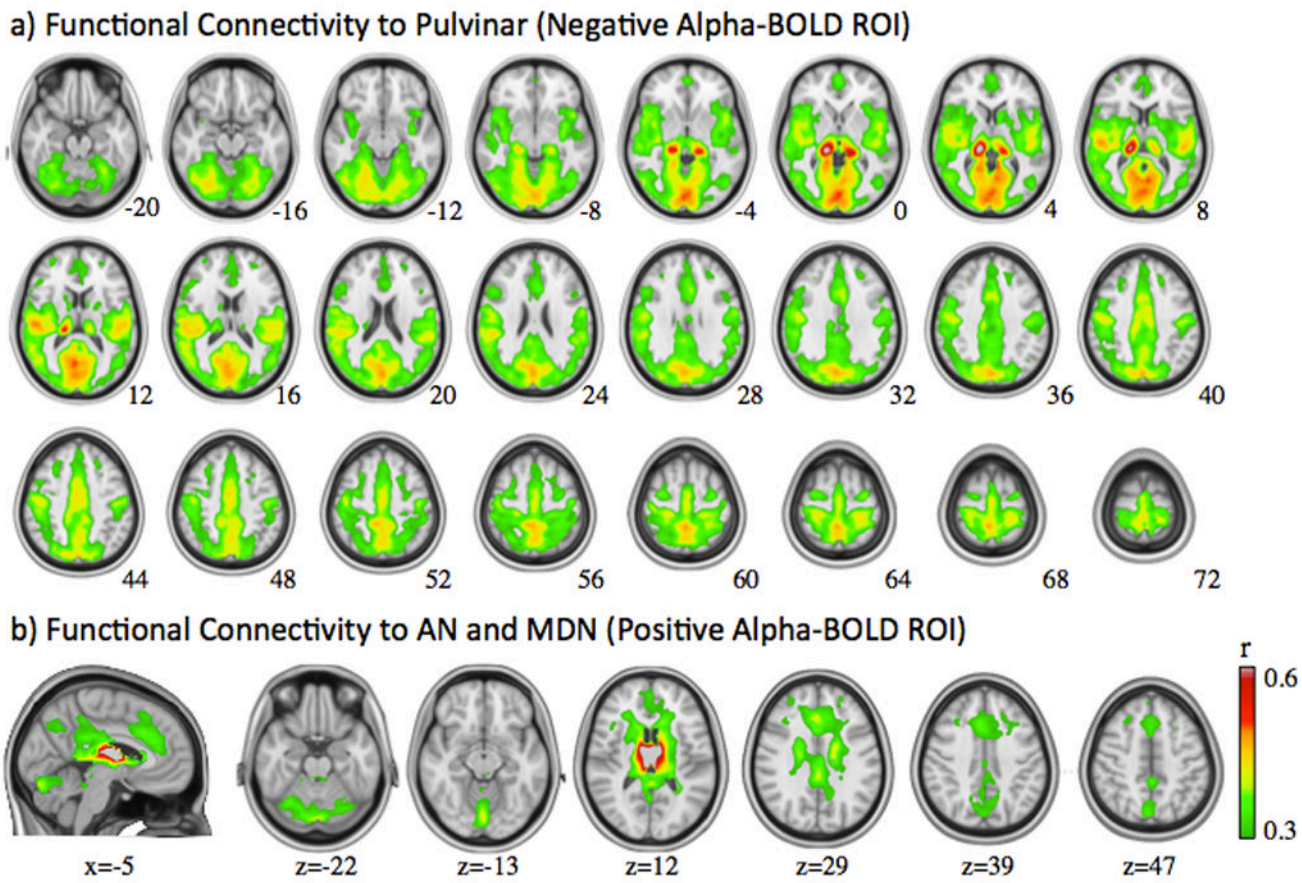


**Figure 6.**
Functional connectivity with the seed region at Pul (a) or AN/MDN (b), as defined from the thalamic regions where BOLD signals are correlated either negatively or positively with posterior alpha power, respectively.